Solid State Phenomena, vols. 82-84, pp. 637-644 (2002)

THE STRUCTURE AND PHOTOLUMINESCENCE OF ERBIUM DOPED NANOCRYSTALLINE SILICON THIN FILMS PRODUCED BY REACTIVE MAGNETRON SPUTTERING

M.F. Cerqueira [1], M. Losurdo [2] M. V. Stepikhova [3] O. Conde[4], M.M. Giangregorio[2], Pedro Pinto[1] and J. A. Ferreira[1]

[1] Departamento de Física, Universidade do Minho, Campus de Gualtar 4710-057 Braga, Portugal

[2] Plasma Chemistry Research Center, CNR, Via Orbona, 4, 70126 Bari, Italy

[3] Institute for Physics of Microstrucutres RAS, 603600 Nizhnij Novgorod GSP-105, Russia

[4] Departamento de Física, Faculdade de Ciência, Edifício C8 Campo Grande 1749-016 Lisboa, Portugal

Keywords: Nanocrystalline silicon, Erbium, Raman, X-ray, Ellipsometry.

Abstract. We have produced and studied undoped and erbium-doped nanocrystalline silicon thin films in order to evaluate the erbium influence on the film microstructure and how this correlates with the photoluminescence properties. Films were grown by reactive RF sputtering. For the doped films metallic erbium was added to the c-Si target. The structural parameters and the chemical composition of the different samples were investigated by X-ray in the grazing incidence geometry, Raman spectroscopy, ellipsometry and Rutherford Back Scattering. The effect of the nc-Si/SiOx matrix ,i.e., nc-Si volume fraction and the presence of SiO and/or SiO_2 phases, on the erbium photoluminescence efficiency is discussed.

Introduction

Both the nanocrystalline silicon (nc-Si) and Er-doped silicon have been attracting enormous interest of researchers as promising candidates for the realization of Si-based visible and infrared light emitters. Moreover the latter takes on special significance for optical communication systems due to the emission line at 1.54 µm (originating by the intra-4f transitions of Er^{3+} ions), which corresponds to the absorption minimum of silica-based glass optical fibers. However, problems arisen in bulk Si:Er operating under forward bias such as the low optical activation of Er centers, as well as the strong temperature quenching of Er emission still remain unsolved. In this context, an improvement can be obtained by incorporation of Er ions in nanocrystalline silicon films [1,2]. This idea is based on the band-gap widening of nanometer size Si, which consequently results in reducing the thermal quenching of Er photoluminescence (PL). On the other hand, Si nanocrystals, that are well known to emit in the visible range [3] due to the recombination of confined excitons within the nanostructure, may act as efficient sensitizers for the rare earth ions. Specifically, it has been demonstrated that, the presence of Si nanocrystals in SiO_2 films drastically (more that 200 times) enhances the 1.54 µm luminescence yield of Er ions [1-4]. Although different models have been proposed to explain the high Er PL efficiency in nc-Si/SiO_2 matrix, the discussion is still open. Debated issues are the nc-Si/SiO_2 interface and the correlation between the nc-Si size and SiOx matrix.

In the present article the effect of the structure/composition of Er-doped nc-Si/SiOx films on the photoluminescence properties is investigated. The peculiarity of this study is the use of spectroscopic

Create PDF files without this message by purchasing novaPDF printer (http://www.novapdf.com)

ellipsometry (SE) to elucidate any correlation between the PL efficiency and the matrix, i.e., the silicon nanocrystallite volume fraction and the SiOx composition. The latter aspect, i.e., the role of SiO and/or SiO_2, can be discriminated because of the sensitivity of SE to the change of the dielectric response of SiOx with change of its stoichiometry. Hence, the correlation between the nc-Si environment and the PL properties is discussed and it is shown that Er PL at 1.54 μm can be also obtained by low density of nc-Si embedded in SiO matrix.

Samples

Erbium doped nanocrystalline silicon thin films were grown by reactive magnetron sputtering on ordinary glass substrates using a procedure similar to that used for the preparation of undoped μc-Si:H films [5]. The target used was a c-Si where for the doping some pieces of high purity (99.99%) metallic erbium were added to the c-Si target. Using this procedure we have grown different samples changing basically the erbium content and substrate temperature. Form our previous work on undoped nanoscrystalline silicon [5] we know that using low RF powers and hydrogen rich atmosphere thin films with silicon nanocrystals are obtained. Table 1 shows, for the samples studied, the growth conditions, the RBS results and the film thickness obtained from the transmission spectra using the Swanepoel [6] and also by ellipsometry. The RF power was kept constant and equal to 80 W during all the experiments (except for Er3 sample that was 40W). All the samples (except Er3 sample) were grown in a hydrogen rich atmosphere, $R_H = 0.63$ ($R_H = pH_2/(pH_2+pAr)$ is the hydrogen fraction). The Er3 sample was grown in a argon rich atmosphere.

Table 1: Growth conditions and sample parameters of undoped (Si#) and erbium doped (Er#) nanocrystalline silicon films. The composition was obtained by RBS. The thickness was obtained by ellipsometry.

Sample	Temperature (°C)	Deposition rate (nm/s)	Thickness (nm)	Er content (%)	O content (%)	Si content (%)
Si13	250	0.029	604	**0**	7	72
Er16	250	0.033	670	**0.07**	5	76
Er13	250	0.037	750	**0.2**	12	88
Er4	250	0.014	285	**0.3**	49	50.7
Si12	350	0.026	540	**0**	5	80
Er20	350	0.043	865	**0.1**	5	76
Er12	350	0.05	857	**0.2**	5	95
Er5	350	<0.01	149	**0.7**	57	42.9
Er3	100	0.065	556	**4.7**	16.3	78
Er19	200	0.013	479	**0.12**	24	62
Er17	400	0.041	871	**0.06**	5	79

From the table we can conclude that the presence of metallic erbium above the silicon target increases the deposition rate except for very thin films.

Structure characterisation

The study of the influence of nanocrystalline size and volume fraction and of the composition and volume fraction of the SiOx on the structure and photoluminescence properties of erbium-doped material has been performed using usual techniques of structural characterization, namely X-ray diffractometry (XRD), and Raman spectroscopy. Moreover, spectroscopic ellipsometry (SE) has been combined with the previous techniques to resolve the film microstructure and composition. In particular, while XRD, Raman and RBS give averaged information on the crystallinity and composition, SE can resolve the film “anatomy”. Thus, the distribution along the film thickness of the volume fractions of the nanocrystalline/amorphous silicon and SiOx phases is obtained. Additionally, on the basis of the different dielectric response of SiO and SiO_2, the presence of the

Create PDF files without this message by purchasing novaPDF printer (http://www.novapdf.com)

two phases can be discriminated. This is achieved through the analysis of spectra of the real, <ε_1>, and imaginary, <ε_2>, parts of the pseudodielectric function, <ε> = <ε_1> + i <ε_2>, acquired in the photon energy range 1.5 – 5.5 eV, by optical models based on the Bruggeman effective medium approximation (BEMA)[7].

X-ray diffraction and Raman spectroscopy. Using X-ray technique combined with Raman spectroscopy information on the crystallinity fraction and the average crystallite size of Si nanocrystals in both undoped and erbium doped samples are obtained.

X-ray diffraction spectra were obtained with a Siemens X-ray Diffractometer D5000 using the Cu K□ line. The sample was measured at grazing incidence (1°). Raman scattering measurements were performed in a Jobin Ivon MicroRaman spectrometer with a triple monochromator using the 514.5nm line of an argon laser. A liquid nitrogen-cooled CCD was used to detect the scattered light. The laser power was kept low enough to avoid modifying the amorphous to crystalline ratio of the samples.

The presence of a nanocrystal fraction in Si:H thin films is clearly evidenced by the characteristic (111) diffraction peaks and Stokes peaks in the vicinity of 520 cm^{-1} observed in X-ray and Raman spectra, respectively.

Figure 1a) shows the X-ray spectra of some representative undoped and Er-doped nc-Si:H thin films, where the three diffraction peaks of c-Si are seen. The relatively large background under the (111) diffraction peak is attributed to the amorphous silicon matrix with some contribution from the glass substrate. It is visible, on Figure 1, both by x-ray and Raman, that the Er19 sample is less crystalline than the others samples.

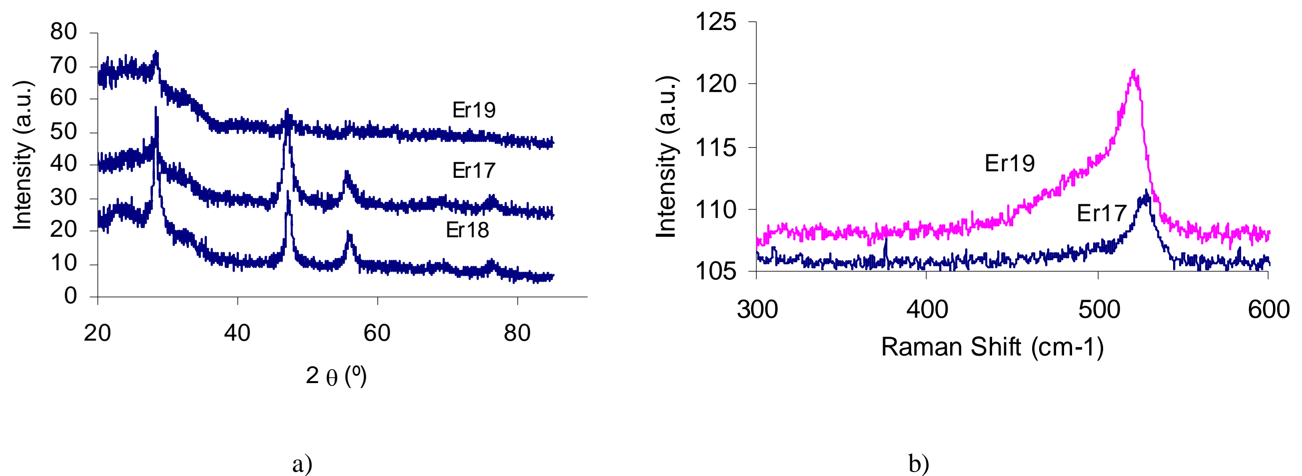

Fig. 1. Typical x-ray (a) and Raman spectra (b) of the some silicon samples produced by reactive RF sputtering.

By fitting a pseudo-Voigt function (pV(x)) to the (111) diffraction peak [8] it is possible to obtain the average crystal size (D) and the thin film strain (ε) of the crystals. From X-ray line profiles, the values for the average grain sizes (D_X) and strain ($\square_X$) obtained are presented in Table 2.

The Raman spectra of some of our samples are shown in figure 1b). To analyse the Raman spectra, we used a Gaussian profile for the amorphous structure (transverse optical mode-TO) and the crystalline profile is calculated based on the Strong Phonon Confinement Model [9,10].

Applying the Strong Phonon Confinement model we obtain the grain size (D_R) and it is possible to calculate the crystalline fraction (c_R) using the integrated intensities of the amorphous and crystalline components [5, 10]. Our results are presented in Table 2.

Create PDF files without this message by purchasing novaPDF printer (http://www.novapdf.com)

Table 2: Samples parameters of grain size (D) and crystalline fraction (c) obtained by X-ray (subscript x) and Raman (subscript R)

Sample	D_x (Å)	ε_x (%)	D_R (Å)	c_R (%)
Si13	96	0.12	71	53
Er16	72	0.09	73	64
Er13	75	0.02	73	75
Er4	Basically	amorphous	material	
Si12	48	0.18	71	66
Er20	56	0.03	80	62
Er12	72	0.06	74	50
Er5	nc-Si	with	low	crystalinity
Er3	Basically	amorphous	material	
Er19	57	0.01	65	43
Er17			78	73

From this table we can verify that the nanocrystals present in the samples without erbium feel a higher strain than the nanocrystals presents in erbium doped samples. We can also verify that the highest substrate temperature will promote crystals with a higher grain size (by Raman).
The sample analysed areas using x-ray diffractometry and Raman spectroscopy are different and thus the information concerning the average grain sizes becomes different. From XRD all the film is analysed and we obtain an average grain size for the three different crystal directions. From Raman spectroscopy we analyse a small area (1 μm^2) and not all the film thickness (due to the sample absorption). Furthermore analysing the Raman spectra we only identify the smallest crystal size (the confined one).

Spectroscopic Ellipsometry. Figure 2 shows experimental and calculated $\langle\varepsilon_2\rangle$ spectra of some typical Erbium-doped samples with different Si and O content (see RBS data in Tab. 1). The calculated best-fit BEMA models are also shown at the bottom of the same figure. Fitting parameters were the volume fraction of constituents and the thickness of each layer. Multilayer structure has been considered because of the presence of in-depth non homogeneous distribution of oxygen; a top SiO_2 layer is also consider to represent the native oxide formed on these surfaces. In order to model data the dielectric function of a-Si [11], nanocrystalline silicon with fine (nc-Si-f) and large (nc-Si-l) [11] grains, of SiO [12], of SiO_2 [11] and of erbium have been considered. As for the dielectric response of erbium in nc-Si/SiOx matrix, it has been measured and derived using a sample with a very large erbium amount. It has been found that SE is sensitive to erbium incorporation into the films even at concentration as low as 0.1 -0.2% and correlates very well with the values obtained by Rutherford backscattering spectroscopy method (see Table 1).
In spectra of fig. 2 two regions can be distinguished, i.e., below bandgap where interference fringes appear, and above bandgap where spectra represent the dielectric response of the composite matrix. In the latter region, it can be seen that the higher the nc-Si volume fraction, the higher the SE spectra and the more evident the two interband critical

Create PDF files without this message by purchasing novaPDF printer (http://www.novapdf.com)

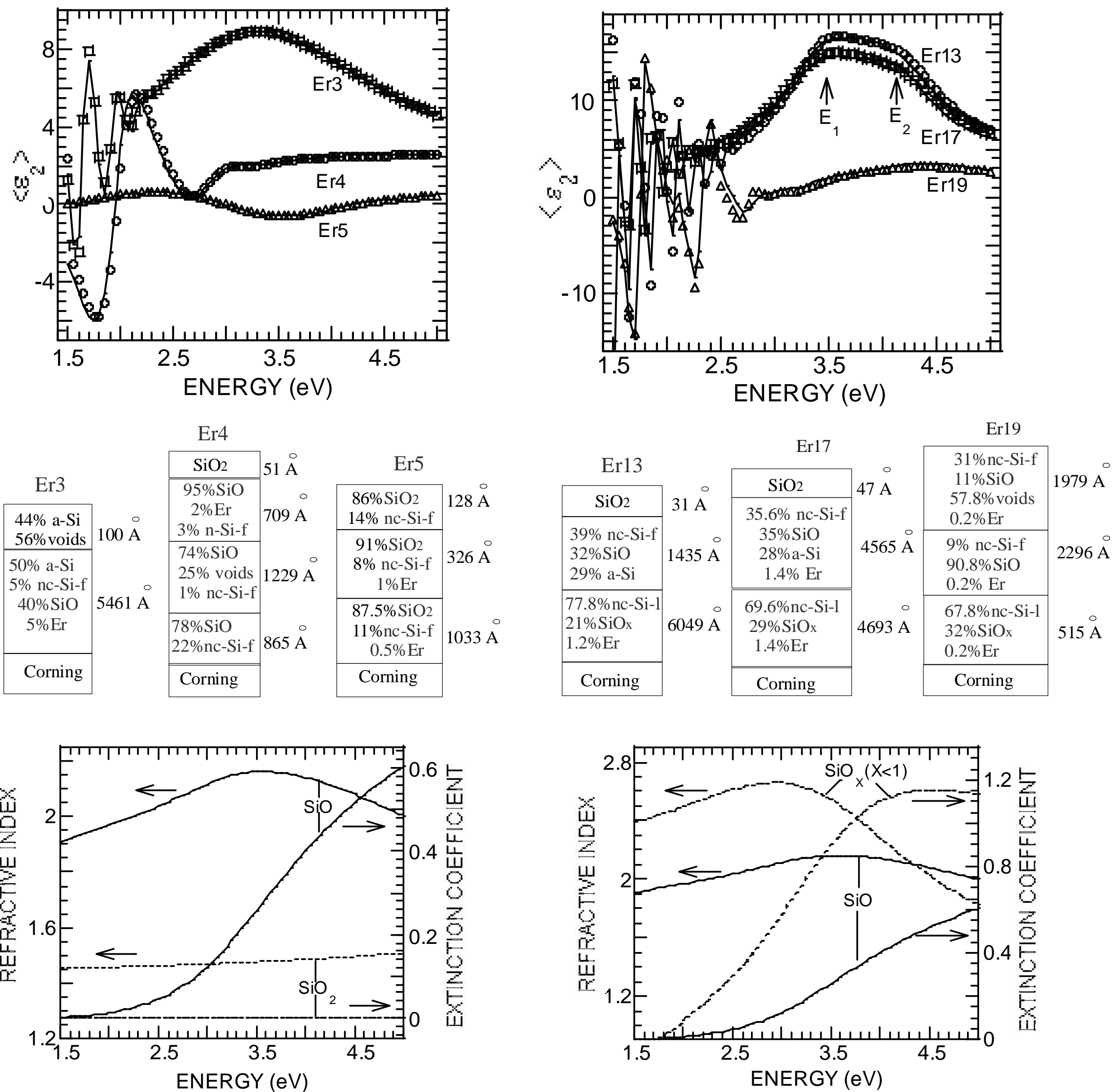

Fig. 2. Typical SE spectra of the imaginary, <ε$_2$>, part of the pseudodielectric function and corresponding BEMA models of Er-doped nc-Si films with different crystalline fraction and SiOx matrix. The best-fit models of each sample are shown at the bottom. The optical parameters (n, k) of the SiO_2, SiO and SiOx (x<1), which enter the fit depending on the grain size, are also shown. SiO and SiO_2 accompany with nc-Si fine grains (nc-Si-f), while SiOx (x<1) accompanies with nc-Si large grains (nc-Si-l).

In spectra of fig. 2 two regions can be distinguished, i.e., below bandgap where interference fringes appear, and above bandgap where spectra represent the dielectric response of the composite matrix. In the latter region, it can be seen that the higher the nc-Si volume fraction, the higher the SE spectra and the more evident the two interband critical point E_1 and E_2 characteristic of c-Si (e.g. Er13, Er17). In contrast, the Er5 sample shows a very low spectrum characterized by the presence of a broad interference fringe, this last indicating that the film is very transparent in all the investigated energy range. Correspondingly, the best-fit model indicates that it is composed of a very small (~ 10%) volume fraction of nc-Si and of Er (~ 0.3%) embedded in a SiO_2 matrix. It can also be seen that the SiO_2 volume fraction increases towards the film surface, i.e. a gradient of oxygen distribution exists. This model agrees with the RBS composition (see Tab. 1), but the further

Create PDF files without this message by purchasing novaPDF printer (http://www.novapdf.com)

information deduced by SE, through the analysis of the dielectric response, is the Si and O bonding configuration, as the SiO_2 phase. A different stoichiometry of the oxide matrix, whose dielectric response has been found to be characteristic of SiO[12] (see fig. 2c) is found for the Er4 sample, in which a larger nc-Si volume fraction (22%) is also detected in the inner layer. Hence, the Er5 and Er4 samples provide good evidence of the sensitivity of SE to not only the SiO_2/SiO phases, but also to the quantification of low nc-Si volume fraction (Er5 and Er4 samples resulted mainly amorphous from XRD and Raman, in Tab. 2). The red-shift of the interference fringes, i.e. the reduced bandgap, and the increase of the spectrum observed for the Er3 sample are consistent with the decrease of the SiO (41%) and nc-Si (7%) volume fractions and with the increase of the a-Si (52%) volume fraction. A 5% of erbium is estimated by SE in agreement with the RBS data. Different features, i.e. higher $<\varepsilon_2>$ values and pronounced E_1 and E_2 critical points characterize the Er17 and Er13 spectra. These features are consistent with a higher nc-Si and a-Si volume fractions than SiO in agreement with the lower O% determined by RBS (when compared to Er4 and Er5 samples). The best-fit BEMA models of these samples consist of a two-layer structure, which stems from in-depth oxygen non homogeneity and surface amorphization, with a native oxide SiO_2 overlayer. In particular, the Er17 has a SiOx volume fraction of ~ 29% in the inner layer which increases to 35% SiO toward the surface. In this surface layer, the Si% is split into a 36% of nc-Si and 28% a-Si phases (the surface amorphization is a consequence of the sputtering process). A lower SiOx volume fraction (21%) in the inner layer with ~ 78 % of nc-Si characterizes the Er13 sample; also in this sample, the SiO volume fraction increases to 32% toward the surface. It is worthy to note that the two layers in the Er17 and Er13 samples differ in the Si crystallite size and oxide phase. In particular, the inner layer has larger Si crystallite grains (n-Si-l) than the outer layer (n-Si-f), and this different grain size is accompanied with a different SiOx phase (see Fig. 2), being SiOx ($x<1$) in the inner layer (with larger grains) and SiO in the outer layer (with fine grains). Therefore, the stoichiometry and bonding configuration of the SiOx matrix relates to the crystallite size of nc-Si. Finally, a different experimental spectrum is found for the Er19 sample whose best-fit BEMA model indicate a SiO% increase but a non homogeneous distribution of SiO and nc-Si phases.

The nc-Si/SiO/SiO_2 distribution and SiOx optical response are useful to explain the photoluminescence properties of the erbium-doped films.

Photoluminescence study

PL spectra for some typical Er doped nc-Si:H thin films are shown in Fig. 3. The characteristic erbium PL at 1.54µm (related to $^4I_{13/2} \rightarrow {}^4I_{15/2}$ transitions of Er ions) is well observable for Er4 and Er5 samples. The Er-related band is well resolved at room temperature and reveals a relatively stable temperature behaviour in contrast to that usually reported for monocrystalline Si. Intensity of PL is quenched only about 3-5 times with increasing temperature from 80 to 300K.This supports the idea that the presence of oxygen is essential for the Erbium PL.

It is evident from data of Fig. 2 and Fig. 3 that the highest PL efficiency is for the Er5 sample which is characterized by a very low volume fraction of nanocrystallites embedded in the SiO_2 matrix (see BEMA model in fig. 2), while the PL in the visible range from nanocrystallites is completely quenched, as already reported by Priolo et al. [1]. However, it is interesting to compare the Er5 and Er4 samples. The latter also shows the Erbium photoluminescence, but with the peculiarity that the very low fraction of silicon crystallites are embedded in a SiO matrix (see BEMA model). The small decrease of PL efficiency observed for the Er4 when compared to Er5 could be explained by the non-homogeneous distribution of nc-Si along the film thickness. However, it should be pointed out that Er photoluminescence can also be observed when nc-Si and Er are embedded in a SiO matrix and not necessarily in SiO_2. As seen for the Er3 sample, a strong decrease of the PL efficiency is observed when the Er concentration and the a-Si volume fractions increase while the volume fraction of SiO decreases. This result can be due to both the erbium concentration quenching [1,2] and the more efficient non-radiative decay related to the large amount of amorphous tissue, hindering the Er ion excitation through the nc-Si. In contrast, when a large nc-Si volume fraction (with small grain

Create PDF files without this message by purchasing novaPDF printer (http://www.novapdf.com)

size) is embedded in the films become strongly absorbing SiO (see Er19), the visible photoluminescence at 714 nm of nc-Si is seen. Here, the auto absorption from nc-Si quenches the Er PL.

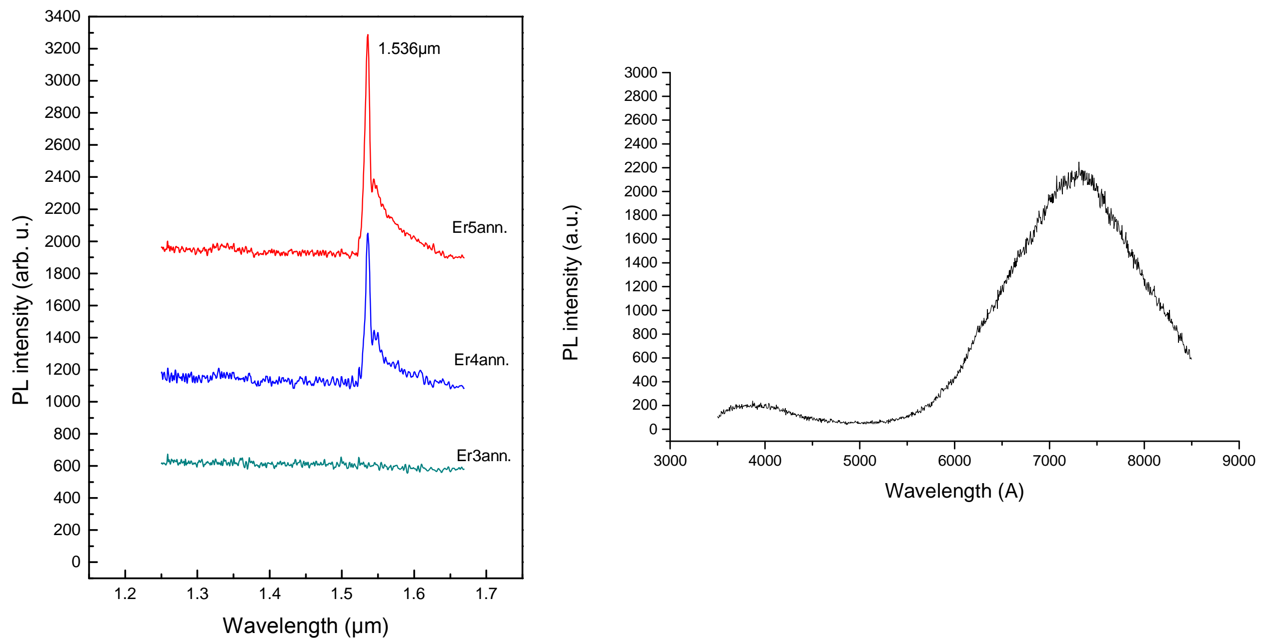

Fig. 3. Er-related photoluminescence spectra of RF sputtered silicon thin films a) Er4, Er5 and Er3 spectra at 5T = 5 K. b) Room temperature PL of Er19 sample.

Summary

It has been shown that structural information, provided by XRD, Raman spectroscopy and spectroscopic ellipsometry, correlates well with photoluminescence properties of erbium-doped nc-Si/SiOx films. In particular, ellipsometry can discriminate the bonding configuration of the oxide matrix, being $SiO_{x<1}$, SiO, SiO_2. We have found that nc-Si embedded not only in SiO_2 but also in SiO promotes Er PL at 1.54 μm, making them suitable to develop nc-Si thin film light emitting devices operating at room temperature.

References

[1] F. Priolo, G. Franzò, D. Pacifici, V. Vinciguerra, F. Iacona, A. Irrora, J. Appl. Phys. 89, (2001) 264.
[2] G. Franzò, D. Pacifici, V. Vinciguerra, F. Priolo, F. Icona, Appl. Phys. Lett. 76 (2000) 2167.
[3] F. Icona, G. Franzò, C. Spinella, J. Appl. Phys. 87, 1295 (2000).
[4] M. Fujii, M. Yoshida, S. Hayashi and K. Yamamoto // J. Appl. Phys. 84, 4525 (1998)
[5] M.F. Cerqueira, M. Andritschky et al. // Vacuum 46, 1385 (1995)
[6] R. Swanepoel, J. Phys. E 16, 1214 (1983)
[7] D.A.G. Bruugeman, Ann. Phys. (Leipzig) 24 (1965) 636.
[8] Th. H. de Keijser, J. I. Langford, E. F. Mittemeyer and A. B. P. Rogels, J. Appl. crystallogr. 11 (1978) 10
[9] M. Yang, D. Huang, P. Hao, F. Zhang, X. Hou, X. Wang, J. Appl. Phys. 75 (1994) 651

Create PDF files without this message by purchasing novaPDF printer (http://www.novapdf.com)

[10] M. F. Cerqueira, J. A. Ferreira, M. Andritschky and Manuel F. M. Costa, Microelectronic Engineering, 43-44 (1998) 627
[11] M. Losurdo, R. Rizzoli, C. Summonte, G. Cicala, P. Capezzuto, G. Bruno, J. Appl. Phys. 88 (2000) 2408 and references therein.
[12] E.D. Palik, Handbook of Optical Constants of Solids II, Academic Press, Inc.San Diego, CA, 1991.

Create PDF files without this message by purchasing novaPDF printer (http://www.novapdf.com)